Desalination and Water Treatment
www.deswater.com

doi: 10.5004/dwt.2017.0056

58 (2017) 181–191
January

Adsorption of phenol from water on activated carbon prepared from shaddock peel by $ZnCl_2$ and H_3PO_4: equilibrium, kinetics and thermodynamics

Bingzheng Li[a,*], Longmei Sun[a], Jianhua Xue[b], Chan Zhang[a], Wei Zheng[a], Liping Zhang[a]

[a]*School of Environment & Safety, Taiyuan University of Science & Technology, Taiyuan 030024, China, Tel. +86 351 6962589; fax: +86 351 6962600; email: bzli@tyust.edu.cn (B. Li), sunlm0214092@163.com (L. Sun), zhang_chan@yahoo.com (C. Zhang), zhwstar2016@163.com (W. Zheng), redzlp@sina.com (L. Zhang)*

[b]*Bei ing Institute of Space Long March Vehicle, Bei ing, 100076, China, Email: xjh0505@163.com (J. Xue)*

Received 14 January 2016; Accepted 1 June 2016

ABSTRACT

The study consists of the preparation of the activated carbon (AC) from shaddock peel by $ZnCl_2$ and H_3PO_4 and the effect of adsorption conditions such as contact time, adsorbent dosage, phenol initial concentration, pH and temperature on the removal behaviors of phenol from aqueous solutions onto the AC. The prepared ACs were characterized by N_2 adsorption, elemental analysis, scanning electron micrograph and Boehm titration. To understand the equilibrium isotherms, the adsorption data were analyzed by Langmuir, Freundlich, Dubinin-Radushkevich and Temkin model. The pseudo-first order, pseudo-second order and intraparticle diffusion kinetic models were used to investigate the kinetic parameters and the mechanism of adsorption. To predict the nature of adsorption, the thermodynamic parameters ($\Delta G°$, $\Delta H°$ and $\Delta S°$) were calculated. The results showed that the micropore structures of two ACs prepared by $ZnCl_2$ and H_3PO_4 activation are similar, but surface chemical properties of different ACs are significantly different. Adsorption removal percentages of ACs for phenol from water increase with increasing the contact time and AC dosage, respectively, whereas phenol removal decreases with an increase in temperature. The changes in the removal of phenol by AC-Z and AC-H with the initial pH were different. The Langmuir and Temkin model can better describe phenol adsorption process for AC-Z; whereas, the Langmuir model can well describe the phenol adsorption process of AC-H. The pseudo-second order and Elovich model better described the adsorption behaviors on AC-H and AC-Z, respectively. The thermodynamic studies indicate phenol adsorption on ACs is spontaneous and exothermic. The experimental results indicate that ACs from shaddock peel by chemical activation methods are technologically feasible. The ACs can be used to effectively remove phenol from wastewater.

Keywords: Adsorption; Phenol; shaddock peel; Equilibrium; Kinetics and thermodynamics

1. Introduction

Phenol and phenolic compounds are aqueous pollutants of high-priority concerns all over the world. Every year, large amounts of phenolic wastewater are discharged from steel mills, coking plants, mineral-processing plants, petroleum refineries, and petrochemical compounds or pharmaceuticals, paints, plywood, coal gas and synthetic resins manufacturers [1,2]. They are toxic and their possible accumulation in the environment will make protein curdle and cause anemia, dizziness and a variety of neurological disorders after inhalation [2]. Hence, phenol in aqueous solutions must be effectively removed before wastewater is sluiced into natural water bodies.

Currently, various technical processes such as oxidation, chemical coagulation, solvent extraction, biodegradation,

* Corresponding author.

distillation, reverse osmosis, precipitation and adsorption have been proposed to remove phenolic compounds from contaminated waters [3]. Among these, adsorption is one of the most important processes. Activated carbon (AC) has been widely used in adsorption operation due to excellent uptake for phenol, which is attributed to huge surface area, developed pore texture and surface chemistry of AC [4,5]. However, due to relatively expensive raw materials such as wood or coal a great number of ACs is not commercially and effectively used to control most pollution. Therefore, it is very important that to effectively reduce AC production costs, researchers are seeking the feasibility of preparation technology of AC from cheaper raw biomass materials. The biomass sources such as forest residues, sugar beet bagasse, agricultural waste material, sunflower seed hull, apricot shell, coconut shell, oil palm fibre, peat, fruit skin, water lettuce and rubber seed coat were used for AC precursor in the references [3,6–8].

China is one of the major shaddock producer countries, and shaddock peel accounts for 44% to 54% total mass of shaddock [9]. Usually, most of shaddock peel is discarded after people eat pulp, while only a small portion is used in medicine production. Zhou et al. studied the adsorption of dyes from aqueous solution by shaddock peel and their results indicated that shaddock peel is rich in porous structure and cellulose and it can effectively adsorb dyes in water [10]. However, the in-depth research regarding the preparation of AC from shaddock peel and its adsorption of phenol in water remains very limited. Therefore, in this work, an attempt was made that ACs were prepared from shaddock peel by $ZnCl_2$ and H_3PO_4 and subsequently main influential experiment parameters of adsorption such as contact time, pH, adsorbent dosage, initial phenol concentration and temperature for phenol removal were studied. And finally the equilibrium, kinetic and thermodynamic data of the adsorption were investigated by different models to describe the adsorption process.

2. Materials and methods

2.1. Materials

2.1.1. Adsorbate and adsorbents

Phenol of analytical grade as an adsorbate was purchased from Beichengfangzheng chemical reagent works (Tianjin, China). It was dissolved in distilled water to yield the stock solution at 1,000 mg L^{-1} and the solution was diluted with distilled water to various different-concentration phenol solutions (1, 5, 10, 20, 30, 50, 100, 200 and 500 mg L^{-1}). $ZnCl_2$ and H_3PO_4 used in the experiments were of analytical grade.

The shaddock peel was collected from the local market. It was pulverized, dried naturally, and then soaked in distilled water to remove surface impurities, dried to constant weight under 60°C in the oven, finally crushed, sieved into particles of 40 to 60 meshes, and stored in a desiccator.

2.1.2. Preparation of activated carbon

Usually, the activation conditions such as chemical activation agent, impregnation ratio, activation temperature and activation time are the main influential parameters of the structure and surface chemistry of activated carbons. Here, $ZnCl_2$ and H_3PO_4 were used as chemical activation agents to activate the biomass samples. And the impregnation ratio and activation temperature in the activation processes were 100 wt.% and 800°C, respectively; whereas, the activation times utilized in $ZnCl_2$ activation and H_3PO_4 activation were 30 min and 60 min, respectively. The specific treatment procedure for the shaddock peel particles was as follows: 6 g of the shaddock peel particles were pre-impregnated by $ZnCl_2$ and H_3PO_4 at 20°C for 12 h, respectively. Afterwards, the samples in a quartz tube reactor of 30 mm in id and 500 mm in length in electronic tube furnace (SRJK-2.5-13, Tianjin, China) were carbonized at 400°C for 1 h with a heating rate of 10°C min^{-1} under a flow of N_2 (99.999%, 50 ml min^{-1}), and the carbonized samples continued to be heated up to 800°C at a rate of 10°C min^{-1} for 30 min and 60 min in N_2 flow of 50 ml min^{-1}, respectively. The activated samples were then cooled to 20°C under N_2 flow. Subsequently, the samples were washed with deionized water to remove possible residual chemicals and some decomposed products until a constant pH in water was reached, dried in the oven at 105°C ± 1°C for 24 h, ground and crushed into particles of 40 to 60 meshes (0.3–0.45 mm) and stored in a desiccator. Shaddock peel was defined as SP and ACs prepared by $ZnCl_2$ activation and H_3PO_4 activation were denoted as AC-Z and AC-H, respectively.

2.2. Characterization of the adsorbents

2.2.1. Chemical composition

The carbon (C), hydrogen (H), and nitrogen (N) contents of the ACs were measured using an elemental analyzer (Elementar Analysensysteme Gmbh Vario EL, Germany). The sulfur (S) content was determined using a sulfur analyzer (SC-132, LECO, USA) and the oxygen (O) content was calculated by the difference.

2.2.2. Texture

Pore structures of the ACs were determined by the N_2 adsorption at 77 K using an automatic ASAP 2020 volumetric sorption analyzer (Micromeritics, USA). The specific surface area (S_{BET}) was determined by the Brunauer-Emmett-Teller (BET) equation. Micropore and mesopore volumes of the adsorbents were calculated by t-plot. The surface morphology of the samples was analyzed using a Japan Instrument JSM-7001F scanning electron microscope (SEM) at accelerating voltages of 3-10 kV.

2.2.3. Surface chemistry characterization

The Boehm titration [5,11] was performed quantitatively and qualitatively to analyze the surface functional groups of AC. It was carried out in 100 mL Teflon bottles containing 0.2 g adsorbents and 25 mL 0.1 mol L^{-1} sodium hydroxide (NaOH), sodium carbonate (Na_2CO_3), sodium bicarbonate ($NaHCO_3$), or hydrochloric acid (HCl) solutions, respectively. The solutions were shaken at 150 rpm at 30°C for 24 h in a thermostatic automatic water bath shaker (SHA-BA, Changzhou, China), then the ACs were separated from the solutions by filtration, and the filtrates were then titrated with 0.1 mol L^{-1} HCl solution or NaOH solution. Phenolphthalein and methyl orange solutions were used as indicators for titration.

The point of zero charge (PZC) is useful for investigating AC's surface charge, which represents the acidic or basic character of the AC surface [12]. It was carried out in 50 mL 0.1 mol L^{-1} NaCl solution in different flasks. The pH was adjusted to a value between 3 and 10 by adding 0.1 mol L^{-1} NaOH or HCl solutions. When achieving a constant pH value, 0.10 g AC was added to each flask and it was shaken for 24 h at room temperature. Blank tests without adsorbents were tested to eliminate the influence of CO_2 on pH.

2.3. Batch adsorption experiments

In batch equilibrium adsorption tests, a series of 50 mg ACs were mixed with 50 mL of phenol solution (100 mg L^{-1}) in sealed glass flasks, then the flasks were agitated in thermostatic water bath shaker at 150 rpm at 30°C for 12 h, and the pH of phenol solution was not adjusted. After adsorption process, the AC was separately filtered from the phenol solutions, and then air dried at room temperature. The equilibrium concentration of the filtrate was measured with a UV-vis spectrophotometer (752N, Shanghai, China) at wavelength of 270 nm for phenol. The equilibrium adsorption capacity (q_e) was defined as the amount of adsorbate per gram of adsorbent in mg g^{-1} and calculated by

$$q_e = \frac{(C_0 - C_e)V}{m} \quad (1)$$

where C_0 and C_e are the initial and equilibrium mass concentrations of phenol (mg L^{-1}) respectively, V is the volume of the solution (L), and m is the weight of the adsorbent (g).

When it was used in this work, the removal percent of phenol by ACs was calculated as follows:

$$\text{Removal (\%)} = \frac{(C_0 - C_e)}{C_0} \times 100\% \quad (2)$$

To investigate the adsorption behaviors of phenol in water on ACs, a series of batch experiments were carried out by amending the adsorptive conditions such as contact time (10–600 min), pH (2–10), adsorbent dosage (0.5–4.0 g L^{-1}), phenol initial concentration (1–500 mg L^{-1}) and adsorption temperature (20°C –50°C). To study the effect of pH, the pH of phenol solution was adjusted with 0.1 mol L^{-1} HCl or 0.1 mol L^{-1} NaOH solutions. The pH was measured by a pH meter (PHS-3C, Shanghai, China).

3. Results and discussion

3.1. Characterization of raw materials and ACs

3.1.1. Chemical composition

The characteristics of SP were presented in Table 1. High carbon and low ash content indicated that the precursor was suitable for AC production. Ash and elemental analyses of the ACs were shown in Table 2. Both ACs had C content far higher than SP, indicating that raw materials (SP) were changed into new materials (AC). It needs to note that C content in AC-H is obviously lower than that AC-Z, but AC-H has the ash content far more than AC-Z, which may be attributed to the over-activation of H_3PO_4.

Table 1
Characteristics of SP

Proximate analysis (%)		Ultimate analysis (%) (dry-ash basis)	
Moisture	8.84	C	41.94
Ash	2.41	H	5.61
Volatiles	71.13	N	0.73
Fixed C	17.62	O	40.40
		HHV (MJ kg^{-1})	14.64

Table 2
Elemental analyses and yield of AC-Z and AC-H

Sample	Ash (wt.%)	C (wt.%)	H (wt.%)	O (wt.%)	N (wt.%)	S (wt.%)	Yield (wt.%)
AC-Z	3.93	82.29	0.83	2.10	2.51	0.09	33.5
AC-H	15.36	69.94	1.50	4.59	0.67	0.03	10.3

Table 3
Textural properties of SP, AC-Z and AC-H

Sample	V_{mic} ($mL g^{-1}$)	V_{meso} ($mL g^{-1}$)	S_{mic} ($m^2 g^{-1}$)	$\bar{r}$ (nm)	S_{BET} ($m^2 g^{-1}$)
SP	0.0004	0.0021	—	4.192	1.69
AC-Z	0.156	0.476	270.613	2.213	1126.01
AC-H	0.162	0.480	287.319	2.518	1005.28

Note: $\bar{r}$ is the average pore width (4V/A by BET).

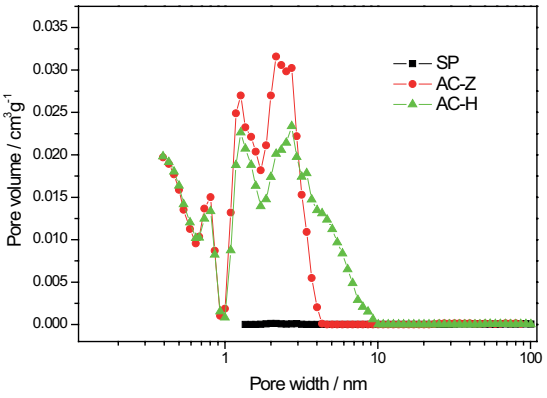

Fig. 1. Pore size distribution of SP, AC-Z and AC-H.

3.1.2. Texture

The textural parameters of SP and ACs were presented in Table 3 and Fig. 1. Obviously, SP has very low pore volume and surface area, which shows that SP itself has almost no pores. Compared with that SP, both AC-Z and AC-H have larger volumes of micropores and mesopores (V_{mic} and V_{meso}) and

the huge surface area (S_{mic} and S_{BET}), showing that ACs have a large number of different types of pores after the activations. It indicates that it is technologically feasible that ACs are prepared from SP by the $ZnCl_2$ and H_3PO_4 activation. From Fig. 1, it is easily seen that there are little differences in the micropore range (V_{mic} and S_{mic}) between AC-Z and AC-H, Here, it needs to be noted that the adsorption capacity of AC for simple organics closely depends on its micropore properties, so according to the data of micropores between AC-Z and AC-H, it is readily obtained that the two activation methods have no major effect on micropores properties of AC. However, AC-H had S_{BET} much lower than that AC-Z, thus showing that AC-Z has the smaller mesopore, which may be subject to the low extent of activation.

SEM micrograph of SP and ACs were given in Fig. 2. Obviously, SP has compact fibrous tissue and a thick-wall structure, which is in agreement with data reported for porous structures in the literature [10]. There are numerous honeycomb-like pores at different sizes and shapes on ACs' surface (Fig. 2 (b) and (c)), indicating that the thick walls of AC surface were opened and accordingly many pores were created after the activation.

3.1.3. Surface chemistry characterization

The acid/base properties of AC-Z and AC-H by Boehm titration and pH_{pzc} were shown in Table 4. Here, the acidic groups of AC surface consist of carboxylic, lactonic and phenolic groups. The acidic groups of AC-H surface were significantly higher than that AC-Z. In Table 4, the pH_{pzc} of ACs was reduced from 6.93 for AC-Z to 6.88 for AC-H, indicating that AC-H had a high acidic character.

3.2. Adsorption of phenol

3.2.1. Effect of contact time

Contact time is an important parameter to determine the time when adsorption reaches equilibrium. Generally, the characteristics of adsorbents and its available sorption sites affected the time needed to reach the equilibrium. Fig. 3 depicted the experimental results for effect of contact time on phenol removal on AC-Z and AC-H. Obviously, adsorption removal increased quickly with an increase in contact time in the initial stages and large amounts of phenol were removed from solutions in 90 min. Both of the contact times needed for AC-Z and AC-H to reach equilibrium were 480 min.

3.2.2. Effect of pH

The effect of initial pH on the adsorption of phenol was investigated within the pH range of 2 to 10. The experimental results for effect of initial pH on phenol removal on AC-Z

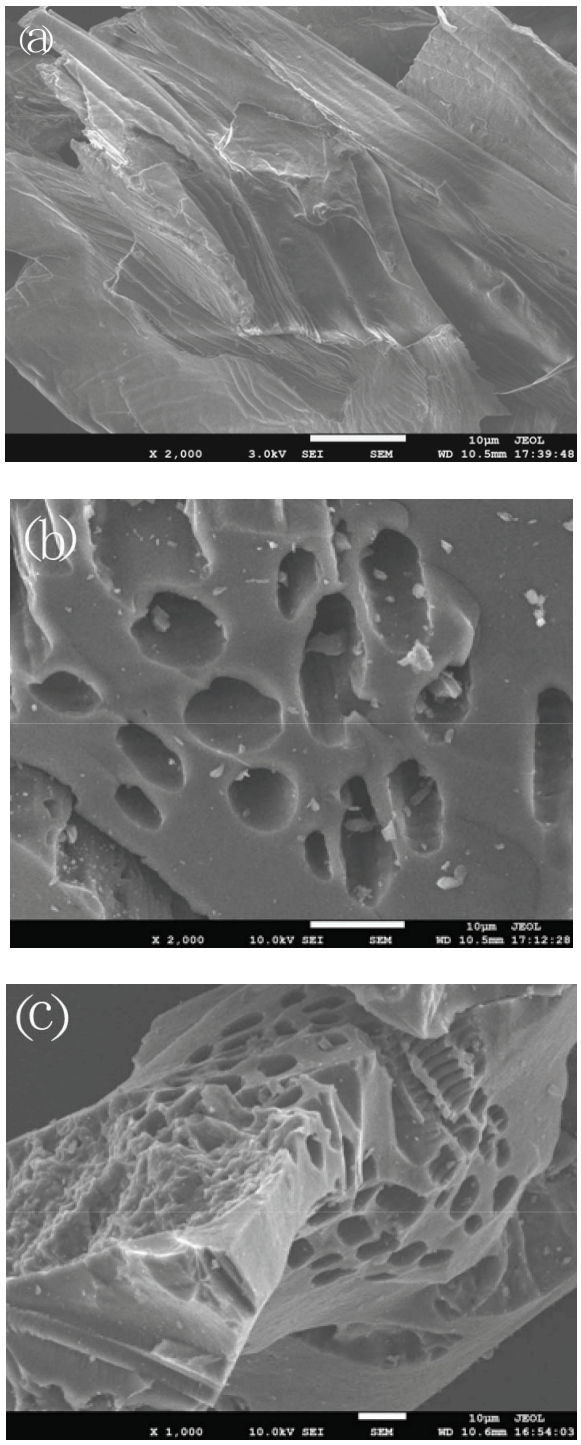

Fig. 2. SEM images of (a) SP; (b) AC-Z; (c) AC-H.

Table 4
Surface chemistry of AC-Z and AC-H

Adsorbent	Acidic groups (mmol g^{-1})	Carboxylic (mmol g^{-1})	Lactonic (mmol g^{-1})	Phenolic (mmol g^{-1})	Basic groups (mmol g^{-1})	pH_{zpc}
AC-Z	3.911	1.813	0.423	1.675	1.485	6.93
AC-H	5.069	2.685	1.275	1.109	0.495	6.88

and AC-H were shown in Fig. 4. Obviously, the changes in the removal of phenol by AC-Z and AC-H with the initial pH were different. The trend of the removal of phenol onto AC-H with increasing pH can be classified into two stages: flat period (pH of 2–8) and rapid decrease period (in the pH range of 8–10). At the flat period, pH in solution has an insignificant effect on the phenol removal, but at the rapid decrease period, the removal rapidly decreased with an increase in pH. However, the phenol removal by AC-Z, with the initial pH of the solution can be divided into three stages: rapid increase period (pH of 2–5), flat period (pH of 5–8) and rapid decrease period (pH of 8–10). When pH in solution increased from 2 to 5, the removal percentage quickly rose; in the pH range of 5 to 8, the removal ratio changed little and the maximum uptake reached at pH 8; The removal percentage rapidly fell when pH increased in the pH range of 8 to 10. This may be due to the difference in the concentrations of H^+ and OH^- in the solutions. AC particles have active sites with negative charges. The H^+ ions within low pH environments can neutralize those negative sites of AC surface, and subsequently reduce a large amount of active sites and finally decrease the chances of their adsorption. High pH environments led to high concentration of OH^-, and phenol mostly exists in ionic state (pH > pKa), so electrostatic repulsion between phenol anions and AC surface occurs, which can increase the inhibition to adsorb phenol [13].

In this work, the initial pH in original phenol solution without adjustment by HCl or NaOH was 6.73. According to the experimental results, the pH in solutions had insignificant influence in the phenol removal in the pH range of 5 to 8, so pH in phenol solutions was not adjusted in the other experiments but the pH experiment.

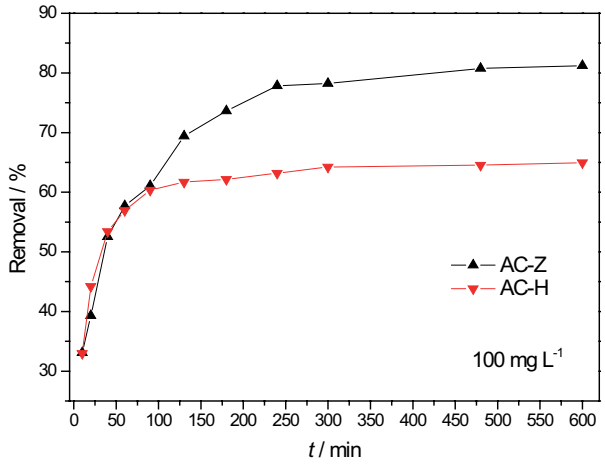

Fig. 3. Effect of contact time on phenol removal onto AC-Z and AC-H.

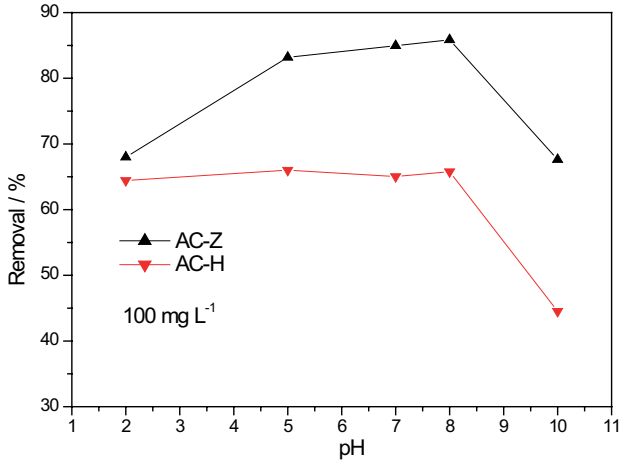

Fig. 4. Effect of pH on phenol removal onto AC-Z and AC-H.

3.2.3. Effect of adsorbent dosage

The adsorbent dosage is an important parameter to investigate the capacity of adsorbent for a given phenol concentration and adsorbate-adsorbent equilibrium of the system [2,14]. The removal percentages of phenol within the range of adsorbent dosage (0.5–4 g L^{-1}) were represented in Fig. 5. Obviously, the phenol adsorption efficiency increases with an increase in dosages of adsorbents up to 2 g L^{-1} and then stabilizes. It is noted that the removal of phenol increased quickly when the dosages of adsorbents increased from 0.5 g L^{-1} to 1 g L^{-1}. This is mainly due to an increase in the availability of the exchangeable sites or surface areas of the adsorbents, resulting in a rise in removal for the adsorption. Considering the cost and availability of ACs, therefore, the optimum amount of AC-Z and AC-H were selected as 1 g L^{-1} in further adsorption experiments.

3.2.4. Effect of initial phenol concentration

The initial concentration provides an important driving force to overcome all mass transfer resistance of phenol between the aqueous solution and solid phase [15]. Fig. 6 showed the results for the adsorption of phenol on AC-Z and AC-H within the concentration range of 1 to 500 mg L^{-1} at 30°C. It could be easily observed that the adsorption behaviors of AC-Z and AC-H for phenol from water were similar. For example, the uptake of phenol on

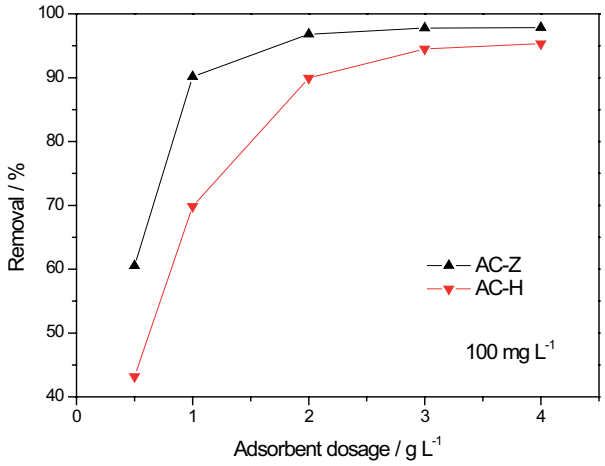

Fig. 5. Effect of adsorbent dosage on phenol removal onto AC-Z and AC-H.

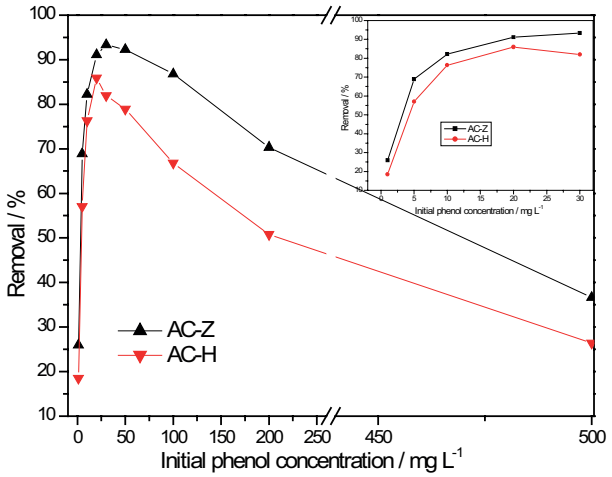

Fig. 6. Effect of initial phenol concentration on phenol removal onto AC-Z and AC-H.

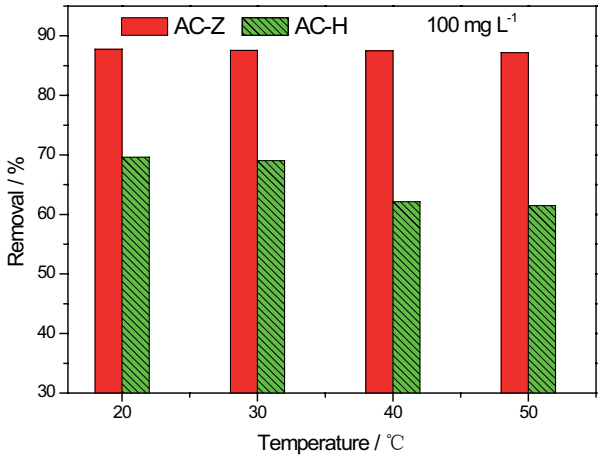

Fig. 7. Effect of temperature on phenol removal onto AC-Z and AC-H.

AC-H increased rapidly with increasing initial phenol concentration up to 20 mg L^{-1}, and then adsorption efficiency relatively slowly decreased with an increase in the initial phenol concentration. One possible reason is that the chance of collision of phenol molecules and adsorbent surface increases, which makes full use of available binding sites on AC within a certain concentration range. Clearly, the maximum removal of phenol by AC-H and AC-Z were 85.93% at 20 mg L^{-1} and 93.33% at 30 mg L^{-1}, respectively. It could be ascribed to the limited adsorption sites provided by the adsorbent surface.

3.2.5. Effect of temperature

Usually, adsorption temperature is an important parameter affecting the adsorptive behavior of adsorbates on the adsorbents. The equilibrium adsorption data of phenol on AC-Z and AC-H at initial concentration of 100 mg L^{-1} with temperatures increasing from 20°C to 50°C were shown in Fig. 7. Clearly, for AC-Z and AC-H, the equilibrium adsorption efficiency decreased slightly with an increase in temperature, indicating that the adsorption processes were exothermic and high experiment temperature was unfavorable for AC-Z and AC-H to adsorb phenol from water. This may be because the more energy was provided in the adsorption process at higher temperature, leading to an increase in the desorption rate from the interface to the solution or the distorted active sites.

3.3. Adsorption isotherms

Langmuir, Freundlich, Dubinin-Radushkevich (D–R) and Temkin isotherm models were frequently used to investigate the adsorption equilibrium of the phenol/adsorbent [16–21].

The Langmuir model is a monolayer adsorption model [16]. The model assumes uniform adsorption on the surface and no transfer in the plane of the surface [17], which can be linearly expressed by

$$\frac{C_e}{q_e} = \frac{C_e}{Q_L} + \frac{1}{K_L Q_L} \tag{3}$$

where the meanings of q_e (mg g^{-1}) and C_e (mg L^{-1}) were the same as Eq. (1); Q_L (mg g^{-1}) is the Langmuir parameter representing the maximum phenol adsorption capacity on the adsorbent; and K_L (L mg^{-1}) is the Langmuir parameter related with the free energy of adsorption.

The Freundlich model [18] is a frequently used adsorption model, which is based on adsorption on heterogeneous surface and active sites with different energy. The linear model can be represented by the following equation:

$$\ln q_e = \ln K_F + \frac{1}{n} \ln C_e \tag{4}$$

where K_F ((mg g^{-1})(L mg^{-1})$^{1/n}$) and n, both empirical constants, are related with the adsorption capacity and the adsorption intensity, respectively. And the value of $n > 1$ indicates a favorable adsorption condition [19].

The Dubinin–Radushkevich (D–R) model [20,21], which is not based on the assumption of a homogeneous surface or constant adsorption potential of AC, is a generally used model to investigate the isotherms of a high degree of rectangularity. This model takes the form of

$$\ln q_e = \ln Q_{D-R} - \beta R^2 T^2 \ln^2\left(1 + \frac{1}{C_e}\right) \tag{5}$$

$$E = \frac{1}{\sqrt{2\beta}} \tag{6}$$

$$T = t + 273.15 \tag{7}$$

where Q_{D-R} (mg g^{-1}) is the theoretical saturation uptake, β (mol^2 kJ^{-2}), a constant, is the mean free energy of adsorption per molecule of the adsorbate when it is transferred to the surface of the solid from infinity in the solution, R (8.314J (mol·K)$^{-1}$) is the gas constant, and T (K) and t (°C) are absolute temperature (a constant for the thermostatic adsorption) and experiment temperature in Celsius degree, respectively. E (kJ mol^{-1}) means the sorption energy, whose values in the

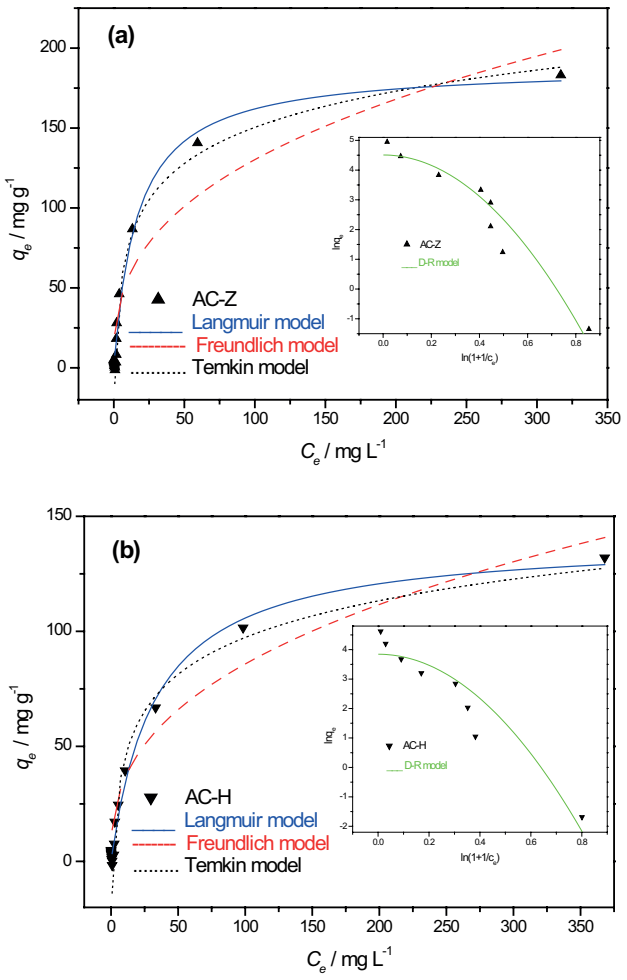

Fig. 8. Adsorption isotherms of phenol on AC-Z and AC-H at 30°C.

range of 8 to 16 kJ/mol would indicate the predominance of an ion exchange mechanism during adsorption [21].

The Temkin model is a decrease in the adsorption heat of all the molecules in the layer in a linear relationship with coverage due to the interaction of adsorbate/adsorbents [22]. The model in linear form can be defined as follows:

$$q_e = F \ln K_T + F \ln C_e \quad (8)$$

where F is related with the heat of adsorption, and K_T (L mg^{-1}), a constant, is the maximum binding energy.

The adsorption data fitted by several models and the models' parameters calculated from the fitting data were shown in Fig. 8 and Table 5, respectively. Both Langmuir and Temkin models fitted well with the experimental data of AC-Z for phenol adsorption, whereas for AC-H, the Langmuir model with the higher correlation coefficient fitted better than Temkin model. According to Langmuir model, the maximum monolayer adsorption capacities of phenol for AC-Z and AC-H were 188.93 mg g^{-1} and 140.50 mg g^{-1}, respectively. Clearly, for the same equilibrium concentration of phenol, the equilibrium adsorption removal of AC-H is

Table 5
Isotherm constants for the adsorption of phenol on AC-Z and AC-H

Isotherms	Parameters	Adsorbent	
		AC-Z	AC-H
Langmuir	Q_L (mg g^{-1})	188.93	140.50
	K_L (L mg^{-1})	0.060	0.031
	R_L	0.14	0.25
	R^2	0.984	0.990
Freundlich	K_F ((mg g^{-1}) (L mg^{-1})$^{1/n}$)	23.98	14.91
	N	2.72	2.63
	R^2	0.894	0.935
Dubinin–Radushkevich	$Q_{D\text{-}R}$ (mg g^{-1})	90.75	46.71
	β	1.37×10^{-6}	1.48×10^{-6}
	E (kJ mol^{-1})	604.1	581.2
	R^2	0.920	0.864
Temkin	K_T (L mg^{-1})	1.00	0.68
	F	32.65	23.09
	R^2	0.987	0.979

significantly less than AC-Z, which is caused by the effect of surface chemistry (mainly oxygen-containing groups) of AC. This can be explained by the mechanism of the π–π interaction. The mechanism is that the π-orbit on the carbon basal planes is interacted with the electronic density in the benzene ring of phenol molecule. The π–π interaction is easily influenced by π-electronic density in the basal plane on AC. Compared with that AC-Z, the stronger deactivating role of more oxygen-containing groups on the AC-H surface reduces π-electronic density in the basal planes of the adsorbents, which makes π–π dispersive interaction weak, and consequently makes its phenol removal decline [23]. In addition, comparing E values (604.1 for AC-Z and 581.2 for AC-H) with the range of 8 to 16 kJ/mol, it was easily obtained that an ion exchange did not occur during phenol adsorption.

3.4. Adsorption kinetics

To understand the adsorption mechanism of adsorbents for phenol, the adsorption kinetics was investigated using pseudo-first-order, pseudo-second-order and Elovich kinetic equation models [24–27].

The pseudo-first-order rate equation of Lagergren, which is considered that the adsorption rate is proportional to the amount of unadsorbed adsorbent surface [24], is expressed by the following equation:

$$\frac{dq_t}{dt} = k_1(q_e - q_t) \quad (9)$$

where q_e and q_t are the amount of phenol adsorbed (mg g^{-1}) at equilibrium and at time t (min), respectively, and k_1 (min^{-1}) is the rate constant of first order adsorption.

The integrated form of Eq. (8) for the boundary conditions $t = 0$ to t and $q_t = 0$ to q_t gives the linear form of the pseudo-first-order rate equation as

$$\ln(q_e - q_t) = \ln q_e - k_1 t \tag{10}$$

Usually, the pseudo-first-order model does not fit well with the whole range of contact time and only describes the initial stage of adsorption [3,25].

The pseudo-second-order model, which is considered that rate-controlling step is based on the chemical adsorption through electronic shared or gain or loss [26], predicts the behavior over the entire range of adsorption. The pseudo-second-order kinetic model equation is given as

$$\frac{dq_t}{dt} = k_2(q_e - q_t)^2 \tag{11}$$

Integrating Eq. (10) for the initial conditions $t = 0$ and $q_t = 0$, gives the following:

$$\frac{t}{q_t} = \frac{1}{k_2 q_e^2} + \frac{t}{q_e} \tag{12}$$

where k_2 is the equilibrium rate constant of pseudo-second-order model (g (mg min)$^{-1}$).

The Elovich kinetic equation, which was widely used in the study of adsorption dynamic behavior and proposed by Elovich in the 1930s, indicated that the adsorption rate decreases exponentially with the increase in the adsorption capacity of the adsorbent surface [4,27]. The model is expressed as follows:

$$q_t = \left(\frac{1}{\beta_d}\right) \ln(\alpha_\alpha \beta_d) + \left(\frac{1}{\beta_d}\right) \ln t \tag{13}$$

where α_a (mg (g min)$^{-1}$) is the initial adsorption rate constant, and β_d (g mg^{-1}) is the desorption rate constant.

The experimental data were fitted with the three kinetic models and the parameters of the kinetic models were given in Fig. 9 and Table 6, respectively. Significantly, the pseudo-second-order kinetic model fitted quite well with the experimental data of AC-H with higher correlation coefficient ($R^2 > 0.99$), which may be due to its description of the whole adsorption process composed of film diffusion, surface adsorption and intraparticle diffusion [15,28]. Whereas phenol adsorption process for AC-Z could be better described by the Elovich model because the correlation coefficient ($R^2 = 0.973$) for AC-Z given by the Elovich model was much higher than that obtained by the pseudo-second-order kinetic model.

The adsorption of phenol appears to be controlled by the chemisorption process. Adsorbate is adsorbed from the liquid phase to the adsorbent particles, which needs to go through the following three steps: film diffusion, inner diffusion and adsorption reaction [15,28]. At first step, the adsorbate diffuses from the aqueous phase to the external surface of sorbent particles through a hypothetical film of fluid. At second step, the adsorbate diffuses from the

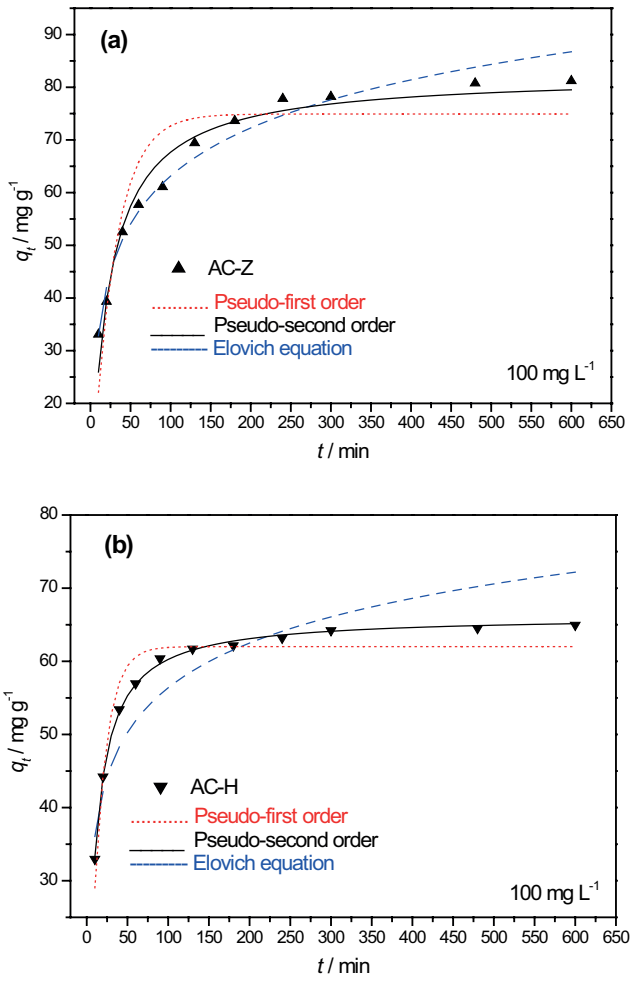

Fig. 9. The fitting of adsorption of phenol in 100 mg L^{-1} on AC-Z and AC-H by Kinetic various models.

Table 6
Parameters of the kinetic models for adsorption of phenol in 100 mg L^{-1}

Kinetic model	Parameters	Adsorbent	
		AC-Z	AC-H
Pseudo-first order	k_1 (min^{-1})	0.035	0.063
	q_e (mg g^{-1})	74.92	62.01
	R^2	0.848	0.936
Pseudo-second order	k_2 (×10^{-3} g (mg min)$^{-1}$)	0.56	1.53
	q_e (mg g^{-1})	82.39	66.22
	R^2	0.964	0.999
Elovich equation	α_a(mg (g·min)$^{-1}$)	15.96	52.50
	β_d (g mg^{-1})	0.076	0.11
	R^2	0.973	0.816

external surface of the particles to the inner surface through the pores of the particles. At third step, the adsorbate molecules are adsorbed on the adsorption sites of the pores. It is well known that the overall rate of adsorption depends on the slowest rate stage of the above process. In general, the third step of the adsorption process reacts quickly and adsorption equilibrium on AC surface is readily attained. Therefore, the total adsorption rate should be controlled by film diffusion and/or internal diffusion. AC as porous materials has rich micropores, mesopores and macropores, which can affect the intraparticle diffusion of phenol into the pores of particle. However, the above three kinetic models cannot on the whole identify the diffusion mechanism and rate-controlling steps that affect the adsorption kinetics. To determine the adsorption rate-controlling step, the particle intraparticle diffusion model is applied to analyze kinetic data of phenol adsorption.

The Weber-Morris intraparticle diffusion equation [18,29] can be expressed as follows:

$$q_t = K_w t^{0.5} + c \tag{14}$$

where K_w is the intraparticle diffusion rate constant (mg (g $min^{0.5})^{-1}$), and c is related to the boundary layer effect.

Weber and Morris believed that the adsorption amount q_t vs. $t^{0.5}$ was linear and passed through the origin, which indicated that intraparticle diffusion was the rate-controlling step. If the plot showed multi-linear characteristic or did not pass through the origin, the adsorption process was controlled by two or more diffusion mechanism [3,30].

The fitting curves of the adsorption data of the adsorbents for the 100 mg L^{-1} phenol by the intraparticle diffusion kinetic model were shown in Fig. 10. Clearly, the plots were not linear over the whole time range, and the q_t against $t^{0.5}$ trend could be classified into three linear parts, i.e., the early adsorption period (predominantly intraparticle diffusion), the middle adsorption period (predominantly film diffusion) and the equilibrium adsorption period. In the initial reaction period, the difference between the phenol concentrations of the aqueous bulk phase and that the adsorbent surface provided a sufficiently strong adsorption force to overcome the external resistance completely, which resulted in a high film diffusion rate; whereas, intraparticle diffusion rate was very low, so intraparticle diffusion was the rate-controlling step in the first stage of adsorption. At the second stage, the adsorption force dependent on the difference in the phenol concentrations of the aqueous bulk phase and the adsorbent surface significantly decreased compared with the early period, so the film diffusion rate obviously reduced and the rate-controlling step was the film diffusion. In the last stage, the adsorption reached almost at equilibrium.

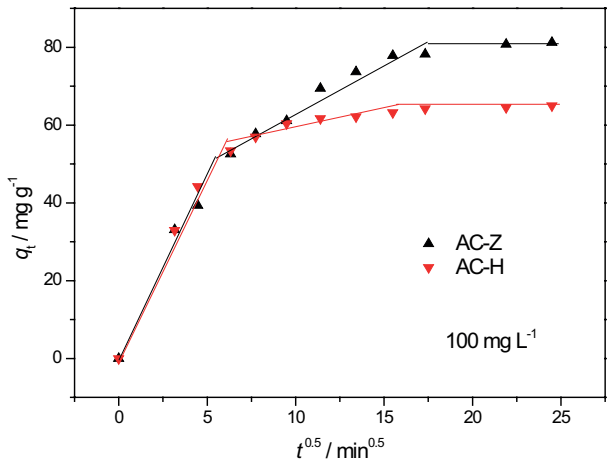

Fig. 10. Intraparticle diffusion plots for phenol adsorbed on AC-Z and AC-H at initial concentration of 100 mg L⁻.

It could also be obtained from Fig. 10 that the total adsorption rate was nearly equal to desorption rate after about 300 min for the ACs. The slopes of AC-H in the intraparticle diffusion-controlling period was slightly lower than that AC-Z, and the result can be attributed to the larger number of acidic groups on the AC surface.

3.5. Adsorption thermodynamics

To investigate of the thermodynamic behavior, several important thermodynamic parameters such as Gibbs free energy change (ΔG°), enthalpy change (ΔH°) and the entropy change (ΔS°), which are often related with adsorption temperature of phenol in the adsorption process, were studied. ΔG° is an important indication of spontaneity of a chemical reaction [31]. ΔH° and ΔS° are two parameters that must be considered in determining the ΔG° of the process. If the value of ΔG° is negative at a given temperature, the reaction will occur spontaneously [31,32].

The value of ΔG° at various temperatures can be calculated from the equations below:

$$\Delta G^o = -RT \ln K_0 \tag{15}$$

where ΔG° (kJ mol^{-1}) is the Gibbs free energy change, K_0 is a thermodynamic constant, which is calculated using the following equation:

$$K_0 = \frac{q_e}{C_e} \tag{16}$$

According to Van't Hoff equation, ΔG°, ΔH° and ΔS° have the linear relation as the Eq. (14)

$$\ln K_0 = -\frac{\Delta G^0}{RT} = -\frac{\Delta H^0}{RT} + \frac{\Delta S^0}{R} \tag{17}$$

where ΔH° (kJ mol^{-1}) is the enthalpy change and ΔS° (J (k $mol)^{-1}$) is the entropy change.

According to the Eq. (16), ΔH° and ΔS° can be calculated from the slope $(-\frac{\Delta H^0}{R})$ and the intercept $(\frac{\Delta S^0}{R})$ of straight line obtained from linear fitting of the plots of $\ln K_0$ versus $1/T$, respectively [31].

According to Eq. (16), The values of q_e, C_e and K_0 were calculated and shown in Table 7 before calculating the thermodynamic parameters ΔG°, ΔH° and ΔS°. And the

Table 7
q_e, C_e and K_0 for the adsorption of phenol on AC-Z and AC-H at different temperatures

t (°C)	AC-Z			AC-H		
	C_e (mg L^{-1})	q_e (mg g^{-1})	K_0	C_e (mg L^{-1})	q_e (mg g^{-1})	K_0
20	12.26	87.74	7.157	30.37	69.63	2.293
30	12.44	87.56	7.038	30.95	69.05	2.231
40	12.52	87.48	6.987	37.85	62.15	1.642
50	12.83	87.17	6.794	38.52	61.48	1.596

Table 8
Thermodynamic parameters for the adsorption of phenol on AC-Z and AC-H

t (°C)	ΔG° (KJ mol^{-1})		ΔH° (KJ mol^{-1})		ΔS° (J $(Kmol)^{-1}$)		R^2	
	AC-Z	AC-H	AC-Z	AC-H	AC-Z	AC-H	AC-Z	AC-H
20	–4.80	–2.03	–1.26	–10.82	12.08	–29.74	0.935	0.865
30	–4.92	–2.02						
40	–5.06	–1.29						
50	–5.15	–1.26						

data of ln K_0 vs $1/T$ were linearly fitted and consequently the values of ΔG°, ΔH° and ΔS° were shown in Table 8. The negative values of the ΔG° at various temperatures (20°C–50°C) indicated the adsorption processes of phenol were spontaneous and feasible. The negative ΔH° values indicated that the nature of adsorption process was exothermic, which theoretically supported the phenomenon that the adsorption capacity of ACs for phenol decreased with the increase in adsorption temperature. However, the values of the $\Delta S°$ were positive (AC-Z) and negative (AC-H), which suggested an increase/decrease in randomness at the solid/solution interface during the adsorption process of phenol on AC, respectively. The difference in the value of $\Delta S°$ could be attributed to the effect of the surface chemistry on the AC surface.

4. Conclusions

The ACs at low cost can be prepared from shaddock peel by $ZnCl_2$ and H_3PO_4 treatment. The micropore structures of two ACs prepared by $ZnCl_2$ and H_3PO_4 activation are similar, but surface chemical properties of different ACs are significantly different.

Adsorption removal percentages of ACs for phenol from water increase with increasing the contact time and AC dosage, respectively, whereas phenol removal decreases with an increase in temperature. The changes in phenol removal of AC-Z and AC-H with pH value of phenol solution are different. It is favorable for ACs to adsorb phenol from water in the pH range of 5 to 8. Phenol removal increases and then decreases with increasing the initial concentration.

The Langmuir and Temkin model can better describe phenol adsorption process for AC-Z; Whereas, the Langmuir model can well describe the phenol adsorption process of AC-H. The pseudo-second order and Elovich model better described the adsorption behaviors on AC-H and AC-Z, respectively. The thermodynamic studies indicate phenol adsorption on ACs is spontaneous and exothermic.

The experimental results indicate that ACs from shaddock peel by chemical activation methods are technologically feasible. The ACs prepared from shaddock peel can be used to effectively remove phenol from wastewater.

Acknowledgements

The authors gratefully acknowledge the financial support from the Research Project Supported by Shanxi Scholarship Council of China (No. 2014-059) and the Undergraduate Innovation and Training Program Fund of Taiyuan University of Science & Technology (No. xj2015051).

Symbols

C_0	—	Initial phenol concentration, mg L^{-1}
C_e	—	Equilibrium phenol concentration, mg L^{-1}
V	—	Volume of the solution, L
m	—	Weight of the adsorbent, g
t	—	Contact time, min
q_e	—	Dadsorption capacity at equilibrium, mg g^{-1}
q_t	—	Adsorption capacity at time t, mg g^{-1}
Q_L	—	Maximum phenol adsorption capacity on an adsorbent, mg g^{-1}
K_L	—	Langmuir parameter related with the free energy of adsorption, L mg^{-1}
K_F	—	Freundlich parameter related with the adsorption capacity, (mg g^{-1})(L mg^{-1})$^{1/n}$
n	—	Freundlich parameter related with the adsorption intensity
Q_{D-R}	—	Theoretical saturation uptake, mg g^{-1}
β	—	Adsorption energy constant, mol^2kJ^{-2}
E	—	The sorption energy, kJ mol^{-1}
R	—	Gas constant, 8.314J $(mol·K)^{-1}$

T — Absolute temperature, K
t — Adsorption temperature in Celsius degree, °C
F — Temkin parameter related with the adsorption heat
K_T — Temkin parameter related with the maximum binding energy, L mg^{-1}
k_1 — Rate constant of pseudo-first order adsorption, min^{-1}
k_2 — Rate constant of pseudo-second order adsorption, g (mg min)$^{-1}$
α_a — Initial adsorption rate constant, mg (g min)$^{-1}$
β_d — desorption rate constant, g mg^{-1}
K_w — Intraparticle diffusion rate constant, mg (g $min^{0.5}$)$^{-1}$
c — Boundary layer effect constant
K_0 — Thermodynamic constant
ΔG° — Gibbs free energy change, kJ mol^{-1}
ΔH° — Enthalpy change, kJ mol^{-1}
ΔS° — Entropy change, J (k mol)$^{-1}$

References

[1] S.H. Lin, R.S. Juang, Adsorption of phenol and its derivates from water using synthetic resins and low-cost natural adsorbents: a review, J. Environ. Manage., 90 (2009) 1336–1349.
[2] S. Mukherjee, S. Kumar, A.K. Misra, M. Fan, Removal of phenols from water environment by activated carbon, bagasse ash and wood charcoal, Chem. Eng. J., 129 (2007) 133–142.
[3] B.H. Hameed, A.A. Rahman, Removal of phenol from aqueous solutions by adsorption onto activated carbon prepared from biomass material, J. Hazard. Mater., 160 (2008) 576–581.
[4] B. Li, K. Sun, Y. Guo, J. Tian, Y. Xue, D. Sun, Adsorption kinetics of phenol from water on Fe/AC, Fuel, 110 (2013) 99–106.
[5] B. Li, Z. Lei, X. Zhang, Z. Huang, Adsorption of simple aromatics from aqueous solutions on modified activated carbon fiber, Catal. Today, 158 (2010) 515–520.
[6] H.I. Chieng, L.B.L. Lim, Namal Priyantha, Sorption characteristics of peat from Brunei Darussalam for the removal of rhodamine B dye from aqueous solution: adsorption isotherms, thermodynamics, kinetics and regeneration studies, Desal. Wat. Treat., 55 (2015) 664–677.
[7] L.B.L. Lim, N. Priyantha, N.H.M. Mansor, Utilizing Artocarpus altilis (Breadfruit) skin for the removal of malachite green: isotherm, kinetics, regeneration and column studies, Desal. Wat. Treat., 57 (2016) 16601–16610.
[8] L.B.L. Lim, N. Priyantha, C.M. Chan, D. Matassan, H.I. Chieng, M.R.R. Kooh, Investigation of the sorption characteristics of Water lettuce (WL) as a potential low-cost biosorbent for the removal of methyl violet 2B, Desal. Wat. Treat., 57 (2016) 8319–8329.
[9] Y. Zhou, C. Hu, J.L. Li, Study on the Biosorption mechanism of methylene blue in aqueous solution using Pummelo peel, Res. Environ. Sci. (in Chinese), 21(2008) 49–54.
[10] Y. Zhou, C. Hu, H. Li, J. Li, H. Zhou, J. Huang, Physico-chemical characteristics of pummelo peel adsorbent, Environ. Sci. & Technol. (in Chinese), 33 (2010) 87–91.
[11] B. Li, Z. Lei, Z. Huang, Surface-treated activated carbon for removal of aromatic compounds from water, Chem. Eng. Technol., 32 (2009) 763–770.
[12] M. Arshadi, M. Mehravar, M.J. Amiri, A.R. Faraji, Synthesis and adsorption characteristics of an heterogenized manganese nanoadsorbent towards methyl orange, J. Colloid Interface Sci., 440 (2015) 189–197.
[13] H. Li, L. Zhang, Z. Sun, Y. Liu, B. Yang, S. Yan, One-step synthesis of magnetic1, 6-hexanediamine-functionalized reduced graphene oxide-zinc ferrite for fast adsorption of Cr (VI), RSC Adv., 5 (2015) 31787–31797.
[14] P. Gridos, A. Dufour, V. Fierro, Y. Rogaume, C. Rogaume, A. Zoulalian, A. Celzard, Activated carbons prepared from wood particleboard wastes: characterization and phenol adsorption capacities, J. Hazard. Mater., 166 (2009) 491–501.
[15] H. Ucun, Y.K. Bayhan, Y. Kaya, Kinetic and thermodynamic studies of the biosorption of Cr (VI) by *Pinus sylvestris* Linn, J. Hazard. Mater., 153 (2008) 52–59.
[16] L. Tang, Y. Cai, G. Yang, Y. Liu, G. Zeng, Y. Zhou, S. Li, et al., Cobalt nanoparticles-embedded magnetic ordered mesoporous carbon for highly effective adsorption of rhodamine B, Appl. Surf. Sci., 314 (2014) 746–753.
[17] N. Wibowo, L. Setyadhi, D. Wibowo, J. Setiawan, S. Ismadji, Adsorption of benzene and toluene from aqueous solutions onto activated carbon and its acid and heat treated forms: Influence of surface chemistry on adsorption, J. Hazard. Mater., 146 (2007) 237–242.
[18] M.S. Sajab, C.H. Chia, S. Zakaria, P.S. Khiew, Cationic and anionic modifications of oil palm empty fruit bunch fibers for the removal of dyes from aqueous solutions, Bioresour. Technol., 128 (2013) 571–577.
[19] M. Kilic, E. Apaydin-Varol, A.E. Pütün, Adsorptive removal of phenol from aqueous solutions on activated carbon prepared from tobacco residues: Equilibrium, kinetics and thermodynamics, J. Hazard. Mater., 189 (2011) 397–403.
[20] Z. Chen, J. Zhang, J. Fu, M. Wang, X. Wang, R. Han, Q. Xu, Adsorption of methylene blue onto poly (cyclotriphosphazene-co-4, 4′-sulfonyldiphenol) nanotubes: Kinetics, isotherm and thermodynamics analysis, J. Hazard. Mater., 273 (2014) 263–271.
[21] Y.S. Ho, J.F. Porter, G. McKay, Equilibrium isotherm studies for the sorption of divalentmetal ions onto peat: copper, nickel and lead single component systems, Water, Air, Soil Poll., 141 (2002) 1–33.
[22] Manasi, V. Rajesh, N. Rajesh, Adsorption isotherms, kinetics and thermodynamic studies towards understanding the interaction between a microbe immobilized polysaccharide matrix and lead, Chem. Eng. J., 248 (2014) 342–351.
[23] R.W. Coughlin, F.S. Ezra, Role of surface acidity in the adsorption of organic pollutants on the surface of carbon, Environ. Sci. Technol., 2 (1968) 291–297.
[24] J. Febrianto, A.N. Kosasih, J. Sunarso, Y.H. Ju, N. Indraswati, S. Ismadji, Equilibrium and kinetic studies in adsorption of heavy metals using biosorbent: a summary of recent studies, J. Hazard. Mater., 162(2009) 616–645.
[25] J.L. Sotelo, G. Ovejero, J.A. Delgado, I. Martínez, Comparison of adsorption equilibrium and kinetics of four chlorinated organics from water onto GAC, Water Res., 36 (2002) 599–608.
[26] I.A.W. Tan, B.H. Hameed, A.L. Ahmad, Equilibrium and kinetic studies on basic dye adsorption by oil palm fibre activated carbon, Chem. Eng. J., 127 (2007) 111–119.
[27] Y. Liu, C. Luo, J. Sun, H. Li, Z. Sun, S. Yan, Enhanced adsorption removal of methyl orange from aqueous solution by nanostructured proton-containing δ-MnO_2, J. Mater. Chem. A., 3 (2015) 5674–5682.
[28] R.L. Liu, Y. Liu, X.Y. Zhou, Z.Q. Zhang, J. Zhang, F.Q. Dang, Biomass-derived highly porous functional carbon fabricated by using a free-standing template for efficient removal of methylene blue, Bioresour. Technol., 154 (2014) 138–147.
[29] H. Li, Z. Sun, L. Zhang, Y. Tian, G. Cui, S. Yan, A cost-effective porous carbon derived from pomelo peel for the removal of methyl orange from aqueous solution, Colloids and Surfaces A: Physicochem. Eng. Aspects, 489 (2016) 191–199.
[30] B. Qiu, C. Xu, D. Sun, Q. Wang, H. Gu, X. Zhang, B.L. Weeks, et al., Polyaniline coating with various substrates for hexavalent chromium removal, Appl. Surf. Sci., 334 (2015) 7–14.
[31] T. Fan, Y. Liu, B. Feng, G. Zeng, C. Yang, M. Zhou, H. Zhou, et al., Biosorption of cadmium (II), zinc (II) and lead (II) by Penicillium simplicissimum: isotherm, kinetics and thermodynamics, J. Hazard. Mater., 160 (2008) 655–661.
[32] S. Kim, T. Yamamoto, A. Endo, T. Ohmori, M. Nakaiwa, Adsorption of phenol and reactive dyes from aqueous solution on carbon cryogel microspheres with controlled porous structure, M. Mesoporous. Mater., 96 (2006) 191–196.